Expression, Purification, and Characterization of Human Factor XIII in *Saccharomyces cerevisiae*

P. D. Bishop,*,‡ D. C. Teller,§ R. A. Smith,‡ G. W. Lasser,‡ T. Gilbert,‡ and R. L. Seale‡

ZymoGenetics, Inc., 4225 Roosevelt Way, N.E., Seattle, Washington 98105, and Department of Biochemistry, University of Washington, Seattle, Washington 98195

Received July 19, 1989; Revised Manuscript Received October 13, 1989

ABSTRACT: Factor XIII is the terminal enzyme of the clotting cascade. A cDNA sequence encoding human placental factor XIII was expressed in *Saccharomyces cerevisiae* with the yeast *ADH2-4*^{c} promoter. Expression levels were a strong function of the noncoding flanking DNA content of the construction. When the terminal 3′-flanking noncoding DNA was removed, expression increased approximately 50-fold. The protein was produced in quantity by high-yield fermentation and purified to homogeneity. The recombinant protein was cleaved by thrombin at the same activation site as purified human placental FXIII and exhibited 100% enzymatic activity. At high thrombin concentrations rFXIIIa was cleaved into inactive 54- and 25-kDa polypeptides. The identity of these cleavage sites and the blocked N-terminus to that of the human protein was revealed by amino acid microsequencing. A time course of thrombin activation was performed and the relative distribution of the thrombin-cleaved subunits to the uncleaved zymogen subunits determined; the results were consistent with the half of the sites catalytic model for transglutaminase activity proposed by Chung et al. (Chung, S. I., Lewis, M. S., & Folk, J. E. (1974) *J. Biol. Chem. 249*, 940–950, 1974) and Hornyak et al. (Hornyak, T. J., Bishop, P. D., & Shafer, J. A. (1989) *Biochemistry 28*, 7326–7332). Equilibrium and velocity sedimentation analysis indicated that rFXIII exists as a 166-kDa nondissociating dimer that behaves as a compact particle of 8.02 S. Thus, all of the properties of rFXIII thus far examined are consistent with those reported for human platelet and placental FXIII. The availability of the recombinant human proteins for therapeutic purposes provides a low-risk alternative to material purified from human sources.

Factor XIII (FXIII)[1] is the last enzyme to become activated in the clotting cascade; its function is to introduce covalent cross-links between noncovalently polymerized fibrin macromolecular complexes [reviewed in Folk (1980), Lorand et al. (1980), and McDonagh (1987)]. Thrombin serves a dual role in the final phase of clotting in that it activates fibrinogen by proteolytic cleavage to fibrin molecules that spontaneously polymerize; simultaneously, thrombin activates FXIII, which then introduces covalent isopeptide linkages between susceptible lysine and glutamine residues of the polymerized fibrin. Cross-linking occurs between fibrin γ-chains, which dimerize, and between fibrin α-chains, which form high molecular weight polymers. These cross-links serve to increase the mechanical stability of the clot and to anchor it to the substratum.

An equally important role of the cross-linking activity is the covalent incorporation of other proteins to the fibrin clot, and to one another. Thus, α_2-plasmin inhibitor is covalently incorporated into the clot and serves to protect it from proteolytic degradation by plasmin, the primary agent of clot lysis (Sakata & Aoki, 1980, 1981; Tamaki & Aoki, 1981; Ichinose & Aoki, 1982). A second protein that is cross-linked to the clot is fibronectin (Mosher, 1975; Mosher & Schad, 1979), serving both to anchor the clot to the tissue substratum and to potentiate macrophage and fibroblast infiltration into the wound site. Other macromolecules reported to undergo cross-linking by FXIII are factor Va, von Willebrand factor, and thrombospondin (Bale & Mosher, 1986; Francis et al., 1986). In some FXIII-deficient individuals, the lack of cross-linking of fibronectin and possibly other macromolecules may be responsible for a high incidence of abnormal wound healing (Duckert, 1972; Bohn, 1978; Lorand et al., 1980).

The FXIII zymogen exists as a heterotetrameric, a_2b_2, complex in plasma and as an a_2 homodimer in platelets, placenta, and other cellular sources (Schwartz et al., 1971; Lorand et al., 1974). The 83-kDa a subunit zymogen contains the cryptic catalytic site that is shared by both molecular forms (Curtis et al., 1974a,b). The b subunit of the plasma zymogen is catalytically inactive and probably serves a carrier, or protective, function (Folk & Finlayson, 1977; Lorand et al., 1980), or regulates activation (Lorand et al., 1974; Chung et al., 1974; Ichinose et al., 1986a; Greenberg et al., 1987). Activation of the zymogen in either form is initiated by thrombin cleavage of a 4-kDa peptide from the N-terminus of the a subunit (Lorand et al., 1964; Schwartz et al., 1971; Tagaki & Doolittle, 1974). In the presence of calcium, the b subunits dissociate from the heterotetrameric circulating complex (Lorand et al., 1974), and the a subunits undergo a conformational change to assume the enzymatically active form (Curtis et al., 1973, 1974a; Chung et al., 1974; Lorand et al., 1974). In this state, the cysteine residues become susceptible to sulfhydryl-reactive reagents such as iodoacetamide (Schwartz et al., 1971; Curtis et al., 1974a; Chung et al., 1974), including the active site cysteine. The proteolytic conversion of fibrinogen to fibrin by thrombin provides poly-

* Correspondence should be addressed to this author.
‡ ZymoGenetics.
§ University of Washington.

[1] Abbreviations: β-ME, 2-mercaptoethanol; DTT, dithiothreitol; EDTA, ethylenediaminetetraacetic acid; FU, fluorescence units; FXIII, human factor XIII; PEG, poly(ethylene glycol); PPACK, D-phenylalanyl-L-prolyl-L-arginine chloromethyl ketone; SDS-PAGE, sodium dodecyl sulfate–polyacrylamide gel electrophoresis; rFXIII, yeast recombinant human placental factor XIII; TANEP, 0.1 M Tris–acetate, 0.15 M NaCl, 1 mM EDTA, and 0.1% PEG, pH 7.5; Tris, tris(hydroxymethyl)aminomethane; Tris–saline, 50 mM Tris and 100 mM NaCl, pH 7.4; YEPGGE, yeast extract (0.1%), peptone (0.05%), D-glycerol (2%), D-galactose (0.1%), and ethanol (2%).

0006-2960/90/0429-1861$02.50/0

meric fibrin, which then serves to potentiate the thrombin activation of FXIII to FXIIIa (Greenberg et al., 1987, 1988; Lewis et al., 1985). When cross-links have been introduced into the polymerized fibrin, thrombin activation is no longer potentiated; this regulatory mechanism apparently serves to provide activated FXIII only when it is needed.

Both subunits of the zymogen have been cloned. The a subunit was cloned by two groups (Grundmann et al., 1986; Ichinose et al., 1986b) and the deduced amino acid sequence matched that of the primary structure of the protein determined by protein sequencing (Takahaski et al., 1986). Although both subunits are found in circulation, only the a subunit is known to exist as an intracellular protein as well as a circulating protein. The secondary modifications of the a subunit indicate it is not processed via the classical secretory pathway; it has an *N*-acetylserine, little or no carbohydrate, and extensive, if not total, free sulfhydryls, and the cDNA does not indicate a signal sequence. The a subunit is present in platelets, megakaryocytes, monocytes, macrophages, spleen, and placenta, but the tissue of origin for circulating a subunit has not been definitively determined (McDonagh, 1987).

Individuals deficient in FXIII have a lifelong tendency toward hemorrhagic episodes characterized by rebleeding following initial clot formation. Children are most critically affected by a high incidence of umbilical and intracranial bleeding, and women deficient in FXIII have a spontaneous abortion rate of 100%. The clinical symptoms can be alleviated by injection of the placental protein at 4–6-week intervals (Kitchens & Newcomb, 1979; Folk, 1980; Lorand et al., 1980; McDonagh, 1987). FXIII has the longest half-life of any clotting factor when administered intravenously, about 12 days (Folk, 1980; Lorand et al., 1980). There is an excess of circulating b subunit, such that injected a_2 subunits become complexed into heterotetramers. Because of the clot-stabilizing effect of FXIII and its involvement in potentiating stability of the extracellular matrix of connective tissue, potential medical applications exist for this protein in wound healing. Toward this end, we have expressed the a subunit of FXIII in the yeast *Saccharomyces cerevisiae*, purified it to homogeneity, and investigated the activation kinetics of the recombinant molecule.

Materials and Methods

Materials. Placental human FXIII was obtained from Alpha Therapeutics (Los Angeles, CA). Bovine and human thrombin were obtained from Enzyme Research Laboratories (South Bend, IN); human FXIII deficient plasma was obtained from CalBiochem (Irwin, CA). [*ring methylene*-^{3}H-(N)]Histamine hydrochloride, 1.2 TBq/mmol (32.1 Ci/mmol), was obtained from ICN Biomedical, Inc. (Costa Mesa, CA). Unless otherwise stated, all other reagents were obtained from Sigma Chemical Co. (St. Louis, MO).

Expression in Yeast. The human placental FXIII *Pst*I coding sequence fragment (Ichinose et al., 1986) was subcloned into cassette vectors containing either the *TPI1* promoter (Alber & Kawasaki, 1982) or the *ADH2-4^c* promoter (Russell et al., 1983) separated from the *TPI1* terminator in both cases by a short polylinker. The expression cassette was then subcloned into a shuttle vector, pEAS101, that contained the *URA3* and the *leu2d* markers. All yeast/*Escherichia coli* shuttle vectors contained the pUC 18 bacterial origin of replication and ampicillin-resistance marker and the yeast 2-μm plasmid DNA containing all intact functions except for coding regions *D* and *FLP*. A polylinker region in the plasmid served to accommodate all constructions described. Several *ura3* or *leu2* yeast strains were transformed and selected for uracil or leucine prototrophy, respectively. The *Pst*I fragment was then subcloned into pUC118 for the purpose of site-directed mutagenesis (Zoller & Smith, 1984) in order to remove 3′-noncoding sequence. An oligonucleotide containing the desired mutation was primer extended (Eghtedarzadeh & Henikoff, 1986) and introduced into *E. coli* strain RZ1032. Mutants were screened by hybridization with the mutagenic oligonucleotide and washed at the T_m for the perfect hybrid, and the mutation was confirmed by dideoxy sequence analysis. The final expression plasmid, pD16, contains the *Schizosaccharomyces pombe* triosephosphate isomerase gene for selection (Thim et al., 1986). The genotype of the final *S. cerevisiae* host strain, ZM118, is *MATa/MaTα Δtpi::URA3/Δtpil::URA3 bar1/bar1 pep4::URA3/pep4::URA3 leu2-3, 112/leu2-3, 112 ura3/ura3* [*cir* °]. Tpi$^-$ cells were grown in YEPGGE for preparation of spheroplasts. Transformants were selected by growth on glucose medium. For high-yield fermentation, an overnight culture of ZM118[pD16] (containing the FXIII gene joined to the *ADH2-4^c* promoter) was inoculated into a stock medium of 25 g/L Difco yeast extract, 22.5 g/L $(NH_4)_2SO_4$, 6.3 g/L KH_2PO_4, 3 g/L $MgSO_4$, and 0.01% (v/v) poly(propylene glycol) in a 12-L New Brunswick fermenter, Model SF116. The initial glucose concentration was brought to 4 g/L at the time of inoculation. Additional glucose was supplied by the continuous addition of a 50% (w/v) solution during the first 46 h of fermentation in order both to maintain exponential growth and to repress FXIII expression. At that point the feed solution was changed to 95% (v/v) ethanol, and growth was allowed to continue for an additional 20 h. The final cell density was approximately 35 g/L dry weight. Extracts were prepared from samples collected throughout fermentation by mixing cells suspended in 50 mM NaCl, 10 mM Tris, and 2 mM EDTA, pH 7.5, with 0.45-μm glass beads and agitating on a vortex mixer at high speed for 3 min. Cell debris was removed by centrifugation and protein content assayed with Bio-Rad (Richland, CA) dye binding reagent and a bovine serum albumin standard.

Radioactivity Assay. The radioactive incorporation assay was a modification of that described by Curtis and Lorand (1976). About 1–2 μg of FXIII from the various stages of purification was activated with 5 units of bovine or human thrombin in 25 μL of reaction buffer (10 mM Tris, pH 7.4, 5 mM DTT) at 37 °C for 30 min. The activation reaction was then stopped with sufficient hirudin, and 60 μL of a reaction mixture containing 7% *N*,*N*-dimethylcasein, 1.35 mM [^{3}H]histamine (34 μCi/mL), 100 mM Tris, pH 7.4, 140 mM NaCl, 10 mM $CaCl_2$, and 5 mM DTT was then added. The reaction mixture was then incubated at 37 °C for 45 min and then stopped by addition of 1 mL of 7.5% TCA. The resulting protein precipitate was then washed twice with 7.5% TCA and dissolved in 100 μL of glacial acetic acid and the incorporated radioactivity determined by scintillation counting.

Fluorometric Activity Assay. A modification of the continuous fluorometric assay first described by Lorand et al. (1971) was performed at 37 °C, as described by Hornyak et al. (1989), using a Perkin-Elmer (Norwalk, CN) LS-5B fluorometer equipped with a jacketed four-cell cuvette holder. All assays were calibrated by adjusting the gain to full scale for a completely reacted sample. Multiple assays were done simultaneously by placing the cuvettes in a Sarstedt Cuvettherm (West Germany) at 37 °C and reading the fluorescence at 5-min time points.

SDS–PAGE and Western Blot Analysis. Analyses of the purification steps were performed with 8% SDS–PAGE, the cross-linking of plasma clots was with 6% SDS–PAGE, and

thrombin activation–deactivation experiments were with 10% SDS–PAGE; all were performed under reducing conditions. The gels were visualized with Coomassive Blue R250 and/or silver stained with a Bio-Rad silver stain kit as described by the manufacturer. For Western blot analysis, the protein was transferred from the gels to nitrocellulose sheets as described by Towbin et al. (1979). The transfers were then incubated with either rabbit anti-FXIII or rabbit anti-yeast antibody and visualized with goat anti-rabbit/peroxidase and HRP substrate as described by the manufacturer (Sigma). All antibodies were diluted with Western buffer A (50 mM Tris, pH 7.4, 5 mM EDTA, 0.05% NP40, 0.15 M NaCl, 0.25% gelatin). Incubations were done at room temperature for 2 h with three 5-min washes between the incubations.

Purification and Crystallization. Purification of rFXIII was carried out as previously described (Hornyak et al., 1989). Unless otherwise stated, all buffered solutions contained 5 mM EDTA and 5 mM β-ME. Cells were harvested, solvent exchanged, and concentrated with a spiral cartridge system (Amicon, Danvers, MA) to yield a final concentration of 50% (packed wet weight to volume) in deionized H_2O. The resulting cell suspension was then diluted with concentrated lysis buffer to give a final cell concentration of 40% in 50 mM Tris-HCl, pH 7.4, 150 mM NaCl, 15 mM EDTA, 5 mM β-ME, and 1 mM phenylmethanesulfonyl fluoride. Cells were lysed in a glass bead mill (DynaMill, Maywood, NJ) using 100-μm acid-washed glass beads. Cell debris was removed from the lysate by centrifugation at 4000*g* for 45 min. The lysate was further clarified by addition of streptomycin sulfate to a final concentration of 2% (w/v) followed by centrifugation at 9000*g* for 60 min. The resulting supernatant was fractionated by addition of PEG-8000 to 8% (w/v) and the precipitate harvested by centrifugation. This crude rFXIII precipitate was then redissolved in 50 mM Tris-HCl, pH 7.8, and applied to a 6 × 27 cm DEAE-cellulose fast-slow Sepharose (Pharmacia-LKB, Piscataway, NJ) column, washed with two column volumes of the same buffer, and the eluted with a linear gradient consisting of 1 L each of buffer A (50 mM imidazole, pH 6.3) and buffer B (50 mM imidazole, pH 6.3, 150 mM NaCl). The peak fractions were then pooled, and the rFXIII was precipitated by dialysis against 50 mM piperazine, pH 6.0. The resulting crystalline precipitate was then redissolved in 50 mM glycine, pH 7.6, and chromatographed on a 4.7 × 80 cm, S-200 Sephacryl (Pharmacia-LKB) column. The peak fractions containing rFXIII were then pooled, filter sterilized, and either used directly or stored lyophilized at 4 °C.

Amino Acid Analysis and Microsequencing. rFXIII samples were first precipitated in 12.5% TCA and then subjected to vapor-phase hydrolysis in 6 N HCl containing 2% phenol for 22 h at 110 °C. The hydrolysate was dried and resuspended in sample diluent (Beckman Na-S buffer) and analyzed with a Beckman (Palo Alto, CA) Model 6300 amino acid analyzer. Microsequencing of thrombin fragments was performed by first separating the fragments by SDS–PAGE, electroblotting onto poly(vinylidene difluoride) membranes, and then directly sequencing on an Applied Biosystems (Foster City, CA) gas-phase sequencer, Model 4000, as described by Matsudaira (1987).

Velocity and Equilibrium Sedimentation. High-speed sedimentation equilibrium experiments using Rayleigh interference optics were performed essentially as described by Teller (1973). The rFXIII solution was dialyzed against 120 mM NaCl, 2.7 mM KCl, and 10 mM phosphate, pH 7.4, at 25 °C. The protein concentration was 1 mg/mL. In the three channels of the Yphantis (1964) style centerpiece the protein concentrations were 0.33, 0.67, and 1.0 mg/mL. Photographic plates were read and processed as described by Senear and Teller (1981).

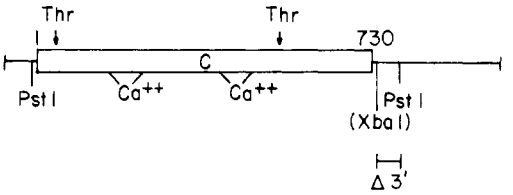

FIGURE 1: Schematic diagram of the FXIII cDNA *Pst*I fragment. The initiator ATG codon is indicated by position 1 and the C-terminal methionine codon by position 730. The coding sequence for the thrombin activation cleavage site is indicated at the N-terminal region and the secondary thrombin site in the carboxy-terminal third of the molecule. Positions of two putative calcium-binding domains elicited by computer analysis (Ichinose et al., 1986b) and the position of the active site cysteine-314 codon are also indicated.

The partial specific volume used was calculated from the amino acid composition according to the revisions of Perkins (1986); the value found was 0.734 mL/g. This was corrected to 5 °C with the factor 3.9×10^{-4} mL g^{-1} deg^{-1} (Pilz & Czerwenka, 1973). The buffer density was calculated to be 1.0044 g/mL at 21 °C and 1.0066 at 5 °C. At each temperature, photographs were taken after 43 h at 13 000 rpm.

Moving-boundary sedimentation velocity experiments were performed in double-sector aluminum-filled epoxy centerpieces in either a six-hole An-G titanium rotor or a four-hold An-F titanium rotor at 48 000 rpm. Sedimentation coefficients were calculated, and the boundaries were fitted for both *s* and *D*.

Plasma Cross-Linking. Samples of normal citrated plasma (pooled from six in-house donors) and FXIII-deficient citrated plasma were diluted 5-fold with 150 mM NaCl and 50 mM Tris-HCl pH 7.4, to give a final fibrinogen concentration of 4 mg/mL. rFXIII was then added to give the desired concentrations, and the samples were clotted by addition of $CaCl_2$ (50 mM final $CaCl_2$) and 0.1 unit/mL thrombin at 37 °C for 6 h. The clots were then harvested by centrifugation at 12000*g* for 1 min, washed twice with saline buffer, and then dissolved by addition of 200 μL of 8 M urea, 1% SDS, 100 mM β-ME, and 50 mM Tris-HCl, pH 6.8, at 60 °C for 16 h. The resulting solutions were then analyzed by SDS–PAGE.

Results and Discussion

Cytosolic Expression in Yeast. The circulating and the cellular forms of the a subunit of FXIII are identical; since the a subunit exhibits characteristics of intracellular proteins (introduction), we decided to express it in *S. cerevisiae* as a cytosolic protein. The cDNA for human FXIII was cloned by Ichinose et al. (1986b) and provided as a subclone in pUC 18. A 2.3-kb *Pst*I fragment encompassing the entire coding sequence (Figure 1) was excised and inserted into two expression cassettes. The first, pRS214, contained the triosephosphate isomerase (*TPI1*) promoter and terminator. The second, pRS215, contained the *ADH2-4*^{c} promoter (Russell et al., 1983) and the *TPI1* terminator. Each expression cassette was then subcloned into a yeast shuttle plasmid containing the *URA3* and *leu2d* (Beggs, 1978) markers. These constructions were transformed into several *ura3* and *leu2* yeast strains and grown for 48 h under uracil (low copy) or leucine (high copy) selection in order to screen for both strain and copy number dependence of expression levels. Cytoplasmic lysates were prepared from each culture, separated by SDS–polyacrylamide gel electrophoresis, transferred to nitrocellulose, and probed with a rabbit polyclonal anti-human FXIII antibody. The results (Figure 2, lanes B and C) showed a barely

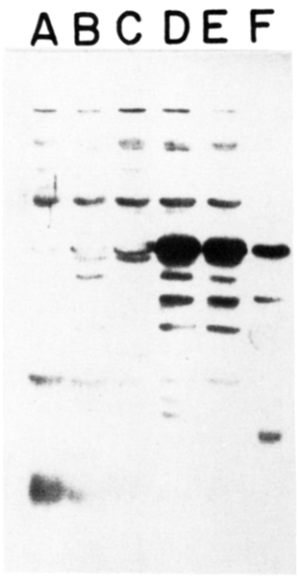

FIGURE 2: Expression of FXIII cDNA. The *Pst*I fragment comprising the entire cDNA sequence plus 5′- and 3′-flanking sequences was cloned into an expression cassette with the *ADH2-4*^{c} promoter and the *TPI1* terminator and expressed in appropriate strains (see text), lanes B and C. Lane A is the control with the vector only. Lanes D and E represent two transformants containing the FXIII DNA following removal of the 3′-noncoding sequence. Lane F is human placental FXIII. 50 μg of yeast protein was loaded in lanes A–E.

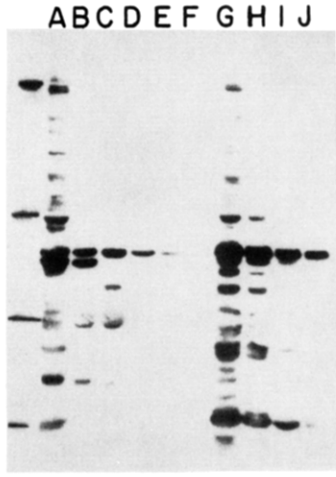

FIGURE 3: Estimation of expression levels in the 3′-deletion expression cassette. Expression levels are shown by Western blotting of SDS–PAGE. Human FXIII was added to lanes C–F in amounts of 0.4, 0.2, 0.1, and 0.05 μg, respectively. Yeast lysate was in lanes G–J in amounts of 50, 25, 10, and 5 μg, respectively. (Lane A) Yeast lysate and (lane B) human human placental FXIII were incubated with thrombin 5 min prior to loading the gel. In the leftmost lane the positions of molecular mass markers for 200, 92.5, 68, and 43 kDa are indicated from top to bottom, respectively.

detectable level of rFXIII protein.

The cDNA *Pst*I fragment employed above had 19 bp of noncoding 5′-flanking sequence and 119 bp of 3′-noncoding sequence. The 5′ sequence both was short and showed significant homology to several AT-rich yeast promoters, including a dA residue at the −3 position (Kozak, 1981). The 3′-noncoding sequence, however, was considerably GC rich, in comparison to yeast DNA, and thus we decided to remove it in order to rule out effects on expression level. An *Xho*I site was introduced immediately 3′ to the TAG codon by oligonucleotide, site-directed mutagenesis (Zoller & Smith, 1984). The DNA was then digested with *Pst*I and *Xho*I, subcloned into the expression plasmid, and retested for expression level as before. The results (Figure 2, lanes D and E) demonstrated a dramatic increase in expression of FXIII protein.

In order to estimate the increased expression, the crude yeast lysate was serially diluted and subjected to electrophoresis along side dilutions of commercially available human placental FXIII. The proteins were transferred to nitrocellulose and probed with anti-FXIII antibody (Figure 3). The sample of 10-fold dilution (lane J) exhibited approximately the same amount of protein as the undiluted standard (lane C). Although quantitation of the protein is not possible by this method due to inherent variation in band intensity, we estimated the level of FXIII in crude yeast culture to be about 50 mg/L, or a 50-fold increase over that in constructions containing the 3′-noncoding sequence. Lanes A and B of Figure 3 show the result of incubation of the recombinant and the human zymogens with thrombin. Both proteins were cleaved to the same extent under these incubation conditions, and the size of the cleaved product appeared to be the same, within the limits of resolution of the gel.

Secretion of rFXIII by Yeast. We were interested in the possibility of expressing the protein through the secretory pathway, for the purpose of ease in purification. Two secretory constructions were prepared. In the first, the yeast α-factor, MFα1, prepro sequence (Kurjan & Herskowitz, 1982) was ligated to the FXIII coding sequence. The 3′ junction of the α-factor prepro sequence occurs at a natural *Hin*dIII site. The 5′ end of the FXIII coding sequence was altered by site-directed mutagenesis in vitro to introduce a *Hin*dIII site in frame with the α-factor sequence, allowing ligation for subcloning into yeast expression vectors. The second secretion construction was prepared by optimizing the invertase signal sequence (von Heijne, 1985, 1986) so as to maximize cleavage at the signal sequence–FXIII junction, by use of two in vitro synthesized complementary oligonucleotides. When these constructions were introduced into yeast on expression plasmids, neither demonstrated secreted FXIII protein into the medium. FXIII protein supplemented to culture medium is stable under these conditions. Therefore, we concluded that FXIII is refractory to production by this method.

High-Yield Fermentation. In order to optimize the expression level of cytosolic rFXIII under high-yield fermentation conditions, cells were grown under conditions of continuous glucose feed so as to allow the accumulation of cell mass in the early production phase, while the promoter was repressed to its lowest expression level. The *ADH2-4*^{c} promoter had a low constitutive activity in the presence of glucose and was induced to a higher level than the wild-type *ADH2* promoter upon exhaustion of glucose from the medium (Russell et al., 1983) and the switch to respiratory growth. During the final phase of fermentation, the promoter was derepressed to its maximal level, and rFXIII product accumulated to the level of approximately 2% of total soluble protein. Figure 4 illustrates the course of rFXIII accumulation during a typical fermentation. The switch from glucose to ethanol occurred between lanes C and D, at which time rFXIII protein was observed to appear. The protein level increased for about 20 h, after which a plateau level was maintained for about 24 h, and then declined (not shown). This level of protein accumulation was lower than that observed for other heterologous proteins expressed into the yeast cytosol (α-1 antitrypsin, placental anticoagulant protein) and is apparently due to toxicity of the a subunit zymogen. For this reason, cytosolic accumulatin of the product was delayed until late in fermentative growth.

Purification. Quantitation and yields of rFXIII obtained

Table I: Quantitation of the Purification Method Developed for rFXIII[a]

step	total protein (g)	total activity (cpm × 10^{-9})	sp act. (cpm/g × 10^{-9})	step yield (%)	total yield (%)
crude lysate[b]	108	250	2.31	100	100
clarified lysate[c]	86.8	190	2.19	76	76
strep SO_4 lysate[d]	71.1	111	1.55	58	44
PEG ppt[e]	26.4	136	5.18	123	54
DEAE[f]	0.735	63.7	86.6	47	25
piperazine ppt.[g]	0.443	75.9	171.3	119	30
S-200[h]	0.315	53.9	170	71	21

[a] Individual purification steps indicated in the left column correspond to the procedures described in the text. PAGE and Western blot analyses of these purification steps are shown in Figures 5–7. All assay procedures are described in the text. [b] Obtained after yeast cell lysis in a glass bead mill. [c] Obtained after low-speed centrifugation of the crude lysate. [d] Supernatant obtained after centrifugation of the streptomycin sulfate treated, clarified lysate. [e] Resolubilized precipitate obtained upon addition of PEG to the streptomycin sulfate treated lysate. [f] rFXIII-containing peak fraction obtained from DEAE-Sephadex chromatography of the resolubilized PEG precipitate. [g] Resolubilized precipitate obtained upon dialysis of the DEAE fraction against piperazine buffer at pH 6.0. [h] rFXIII-containing peak fraction obtained from gel filtration chromatography of the resolubilized piperazine precipitate.

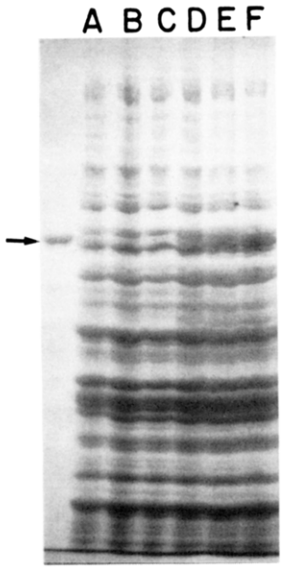

FIGURE 4: High-yield fermentation of yeast for FXIII production. Yeast FXIII production is shown by a Coomassie Blue stained SDS–PAGE of samples taken from a 12-L culture of strain ZM118[pD16] grown with a two phase fed batch growth regime (Materials and Methods). Extracts were prepared from samples collected throughout the experiment and cell lysates prepared. Lanes A–F each contain 0.1 mg of total cell protein and represent a time course of the fermentation. Lanes A–C are from the glucose growth phase at 26, 32, and 44 h after inoculation, respectively. Lanes D–F are from 5, 10, and 20 h after the switch to ethanol growth at 4 h. The leftmost lane contains 5 μg of purified FXIII.

Table II: Amino Acid Composition of rFXIII

amino acid	mol % determined[a]	mol % expected[b]	residues per 83.0 kDa determined[c]	residues per 83.0 kDa expected[b]
Asx	12.58 ● 0.08	12.32	85.6 ● 1.4	87
Thr	6.03 ± 0.12	6.37	46.0[d]	45
Ser	5.57 ● 0.60	6.52	48.3[d]	46
Glx	10.70 ● 0.77	10.62	72.8 ● 5.6	74
Pro	4.62 ● 0.24	4.67	31.4 ± 1.6	33
Gly	7.54 ± 0.34	7.08	51.2 ● 2.0	50
Ala	5.63 ± 0.25	5.24	38.3 ± 1.8	37
Val	9.84 ± 0.36	10.06	71.2[d]	71
Met	2.30 ● 0.41	2.55	15.7 ● 3.0	18
Ile	5.06 ● 0.15	5.38	37.7[d]	38
Leu	7.12 ● 0.18	6.8	48.5 ● 1.1	48
Tyr	4.01 ± 0.11	4.11	27.3 ± 1.0	29
Phe	4.60 ± 0.11	4.53	31.3 ± 0.6	32
His	2.05 ● 0.10	1.98	13.9 ± 0.5	14
Lys	5.54 ● 0.16	5.38	37.7 ± 0.7	38
Arg	6.81 ± 0.25	6.37	46.4 ● 1.3	45

[a] The value of each amino acid is given as the mean ± standard deviation (moles of amino acid per 100 residues) for seven samples. Hydrolysis conditions are described under Materials and Methods. Data *were not* weighted and hydrolytic errors for serine, threonine, valine and isoleucine *were not* corrected. [b] Expected values were calculated on the basis of the amino acid composition derived from the cDNA sequence corrected for 9 cystiene and 15 tryptophan residues per mole of rFXIII. [c] The value of each amino acid is given as the mean ± standard deviation (for seven samples). Values *were weighted* to give the best fit (i.e., by the average R value of each run) for alanine, phenylalanine, leucine, lysine, arginine, histidine, aspartic acid (Asx), and glutamic acid (Glx). [d] Hydrolytic errors for serine, threonine, valine, and isoleucine were corrected by performing a time series hydrolysis (24, 48, 72, and 96 h) and extrapolating to obtain the maximum molar yields.

during a typical purification run are shown in Table I. The apparent anomalies in the recoveries of rFXIII (i.e., yields greater than 100% obtained upon precipitation with PEG or piperazine buffer) are apparently due to inhibitors present in the preceding purification steps that lead to underestimation of the enzymatic activity. The final purification step (S-200 gel filtration) did not result in a detectable increase in rFXIII specific activity but was necessary for the removal of trace amounts of uncharacterized high molecular weight material. The final yield of rFXIII obtained from the crude lysate determined over the course of five typical purification runs has been determined to be 26 ± 5%.

Each step of the purification was monitored by 8% SDS–PAGE gels with 20 μg of total protein per lane. Proteins were visualized by staining with Coomassie Blue R250 to estimate the relative abundance of each band and then silver stained to enhance minor bands (Figure 5A). Western blotting using anti-human FXIII was used to identify the rFXIII band and to detect the presence of rFXIII fragments in the preparation; the 83-kDa a subunit was clearly evident, and a small amount of a 68-kDa contaminant band (below the level of detection in the silver-stained gel) was also present in the S-200 preparation (data not shown). The extent of contamination by yeast proteins was further examined by Western blotting with antibodies raised against whole yeast cytosolic extracts (Figure 5B). No detectable yeast proteins were found following the piperazine precipitation step (crystallization). Further evidence of purity comes from the observations of Hornyak et al. (1989), which show that rFXIII has an identical specific activity with that of purified human platelet FXIII. We therefore estimate that the final purified preparation was ~99% rFXIII.

Amino Acid Analysis. The amino acid analysis of purified rFXIII is given in Table II. The composition is within experimental error of the composition predicted from the cDNA and agrees well with that reported by Bohn (1970). The amino acid composition was found to be very consistent between individual purification runs.

Sedimentation Analysis. Sedimentation equilibrium experiments were performed in order to monitor the physical

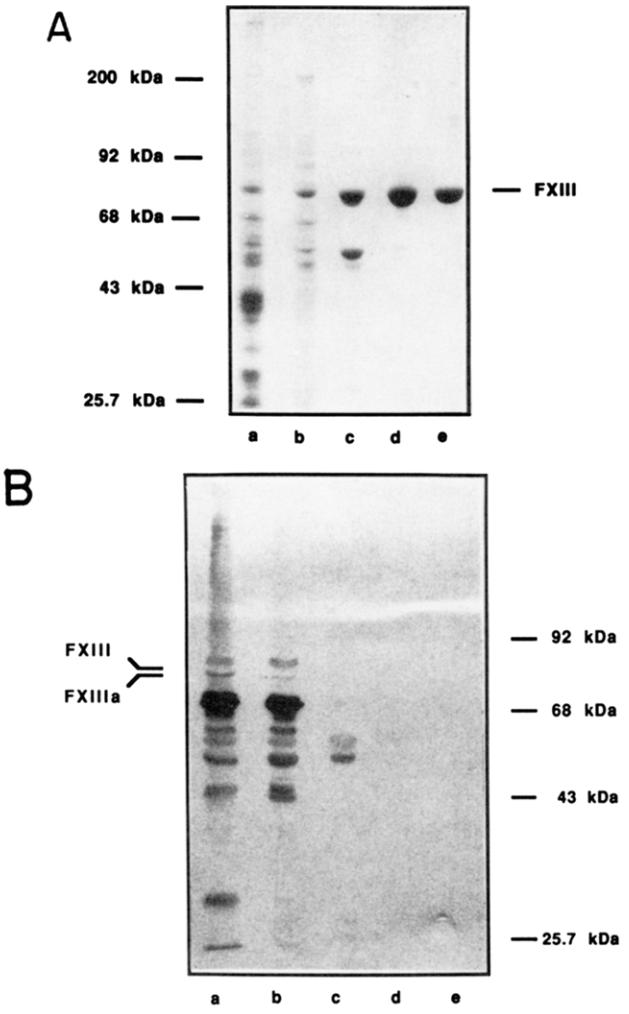

FIGURE 5: PAGE and anti-yeast protein Western blot analysis of the purification method for rFXIII. Panel A: Fractions that are representative of the purification scheme outlined in the text are compared by reducing SDS–PAGE. Lane a, clarified yeast lysate; lane b, PEG-8000 precipitate; lane c, DEAE-Sephadex chromatography; lane d, piperazine precipitation; lane e, S-200 gel filtration chromatography. Each lane was loaded with equivalent amounts of total protein. The gel was first stained with Coomassie Blue in order to give an indication of the relative abundance of rFXIII in each fraction and then silver stained to enhance visualization of minor impurities. Panel B: The same fractions that were shown in panel A are compared by anti-yeast protein Western blotting of reducing SDS–PAGE. Lane a, clarified yeast lysate; lane b, PEG-8000 precipitate; lane c, DEAE-Sephadex chromatography; lane d, piperazine precipitation; lane e, S-200 gel filtration chromatography. Each lane was loaded with equivalent amounts of total protein. See text for experimental details.

state of the rFXIII zymogen. We attempted to fit the data to a monomer–dimer system, but that model fitted only two of the five sets of data. The lack of a monomer–dimer fit to the data means that no dissociation of the dimer occurs above 0.1–1.0 μg/mL in protein concentration. The variance weighted average of a fit of the data to a single component gave 166 000 ± 800 g/mol as the molecular mass of the single component, exactly twice the molecular mass determined by Takahashi et al. (1986) and Ichinose et al. (1986b) for a monomeric subunit. We conclude that no dissociation of dimeric rFXIII occurs in solution.

In order to calculate the frictional coefficient and the Stokes radius of the rFXIII molecule, sedimentation velocity experiments were performed. The initial s vs C dependence was determined in 0.15 M NaCl and 0.05 M Na_3PO_4, pH 7.25, at 20 °C in the six-hole rotor. The results of this experiment gave $s^0_{20,w}$ = 8.02 S.

Table III: Summary of the Physical Properties of Recombinant Factor XIII Determined by Analytical Ultracentrifugation[a]

molecular weight, MW (n = 15, no. of samples = 3)[b]	166 000 ± 800
sedimentation coeff, $s^0_{20,w}$ (n = 27, no. of samples = 7)	8.02 ± 0.11
frictional coeff, $f_{20,w}$ (g/s)	(9.20 ± 0.13) × 10^{-8}
Stokes radius, R_s (Å)	48.7 ± 0.07
frictional ratios	
$(f/f_0)_{obs}$	1.337 ± 0.018
$(f/f_0)_{shape}$[d]	1.114 ± 0.015
dimer of touching spheres, $(f/f_0)_{shape}$[e]	1.1049
subunit axial dimensions (Å)[f]	
prolate	a = 35.3; b = 26.1
oblate	a = 23.6; b = 32.0

[a] (±) refers to standard deviation. Values in the table are extrapolated to zero concentration. [b] Molecular weight determined by equilibrium sedimentation in PBS, pH 7.4, at 21 and 5 °C. $\bar{v}$ (0.734 mL/g) was determined from the amino acid composition of rFXIII as described by Perkin (1986). [c] Sedimentation coefficient determined in 50 mM NaH_2PO_4 and 150 mM NaCl, pH 7.4, at 20.74 °C. [d] Corrected for rugosity (hydration) (Teller et al., 1979). [e] deHaen et al., 1983; Swanson et al., 1980. [f] The axial dimensions of a subunit are calculated from the anhydrous volume (101.2 × 10^3 Å^3) and f/f_0 = 1.008 = 1.114/1.1049. Equation 103 from Perrin (1936) was used for the shape factor.

The finding that the sedimentation coefficient was 8.02 S in phosphate buffer for the rFXIII protein, rather than lower value of 7.3 S recently reported (Carrell et al., 1989), prompted us to examine the protein under conditions similar to those of Carrell et al. (1989). Two moving-boundary experiments were run at identical protein concentrations (0.23 mg/mL). The solutions were dialyzed against Tris–saline, pH 7.50 (20 °C), and one sample was made 10 mM in $CaCl_2$ while the other was 1 mM in EDTA. There was essentially no difference between these two samples in sedimentation coefficient (7.96 and 7.95 S, respectively), nor was there a difference from the samples in phosphate buffer.

Table III summarizes the ultracentrifugation results on the rFXIII protein. The salient features are as follows: First, the protein is physically homogeneous, with no evidence for dissociation, as has been reported for the platelet protein by others (Chung et al., 1974; Schwartz et al., 1973). Second, the sedimentation coefficient of 8.02 S yields a Stokes radius of 48.7 ± 0.7 Å, and $(f/f_0)_{obs}$ = 1.337 ± 0.018. To obtain the shape of the dimer, we corrected the observed friction ratio by the factor 1.2 (Teller et al., 1979), which yields $(f/f_0)_{shape}$ = 1.114 ± 0.015. The best estimate of the shape factor for a dimer of touching spheres is that of the extrapolated shell model (deHaen et al., 1983; Swanson et al., 1980), which gave $(f/f_0)_{shape}$ = 1.1049. It is clear that the recombinant rFXIII fits this shape within 1%. Thus, in contrast to the recent report of Carrell et al. (1989) we do not see elongation of the subunits in our preparation of rFXIII but instead observed a very compact dimer.

Thrombin Activation and Inactivation of rFXIII. Thrombin rapidly catalyzes the cleavage and release of a 4-kDa amino-terminal activation peptide from the stable FXIII zymogen to yield FXIIIa enzyme. A second thrombin cleavage can also occur on the 79-kDa enzyme leading to the formation of 25- and 54-kDa fragments, which probably inactivates FXIIIa (Takahaski et al., 1986). Figure 6 shows the SDS–PAGE analysis of equal quantities of rFXIII incubated with varying concentrations of thrombin. It is clear from this figure that the sensitivites of the cleavage sites toward thrombin differ greatly. The product of the thrombin concentration and incubation time required to effect the second thrombin cleavage (i.e., production of 25- and 54-kDa fragments) was approxi-

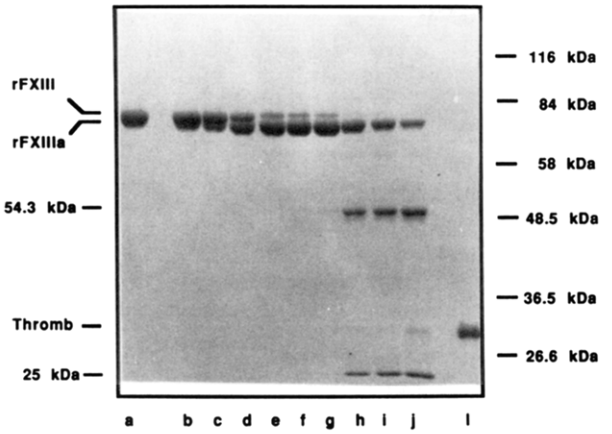

FIGURE 6: Thrombin activation and inactivation of rFXIII. rFXIII (0.67 mg/mL in Tris–saline) was subjected to cleavage by bovine thrombin. The following samples were incubated with the indicated amounts of thrombin: (a) 0 (rFXIII alone); (b) 0.13 unit/mL thrombin; (c) 0.27 unit/mL; (d) 0.53 unit/mL; (e) 1.3 units/mL; (f) 2.7 units/mL; (g) 5.3 units/mL; (h) 13 units/mL; (i) 27 units/mL; (j) 53 units/mL. Samples b–g were incubated for 30 min at 37 °C and samples h–j were incubated for 7 h at 37 °C. Sample l is bovine thrombin standard.

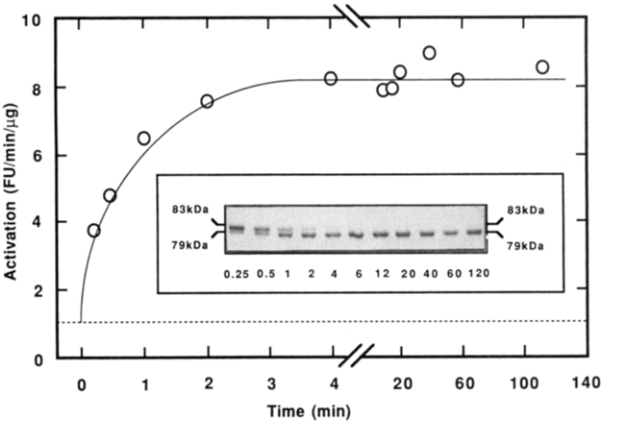

FIGURE 7: Time course of rFXIII activation by thrombin. rFXIII (0.5 mg/mL) was activated by human thrombin (5×10^{-3} unit/mL) in TANEP buffer containing 14 mM $CaCl_2$ at 37 °C for the times indicated. The activation reaction was stopped by inhibiting thrombin with PPACK (3 μM final concentration). Activity was then immediately assayed by monitoring the rate (fluorescence enhancement) of the rFXIII-catalyzed incorporation of dansylcadaverine into *N*,*N*-dimethylcasein (see Materials and Methods). The dashed line indicates the non-thrombin-activated background rate of pure a_2 dimer in the presents of 14 mM Ca^{2+} (Ca^{2+} background). The relative distribution of the a (83 kDa) and a′ (79 kDa) subunits was determined by SDS–PAGE (photo inset) for the various states (times) of activation shown.

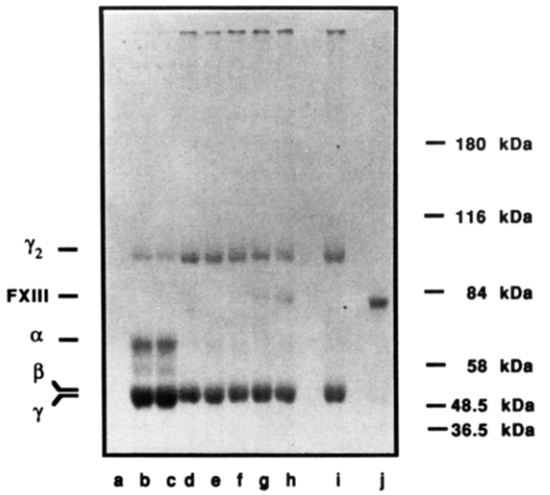

FIGURE 8: rFXIII cross-linking in clots derived from FXIII-deficient plasma. Reducing SDS–PAGE of solubilized human FXIII deficient clots (a–h) is compared to normal human plasma (i). Citrated plasma was diluted 5-fold with isotonic Tris–saline buffer, and the following samples were supplemented with rFXIII: (a–c) none; (d) 2 μg/mL; (e) 4 μg/mL; (f) 10 μg/mL; (g) 20 μg/mL; (h) 40 μg/mL. Plasma samples (except a) were then recalcified to give 10 mM Ca^{2+} excess over citrate and supplemented with 0.1 unit/mL bovine thrombin (except b). The samples were then allowed to clot for 6 h at 37 °C (note that a did not clot) and then centrifuged to remove nonclotting proteins. The clots were then washed twice with buffer and then dissolved in 0.1 M β-mercaptoethanol, 1% SDS, and 8 M urea for 16 h at 60 °C and centrifuged to remove insolubles. Equal volumes of the resulting solutions were then analyzed by 6% SDS–PAGE. Note that samples d and e received an amount of rFXIII functionally equivalent to the amount FXIII present in normal plasma (samples i); i.e., 10–20 μg/mL. Lane j contained rFXIII standard.

mately 1000-fold greater than was required for the activation cleavage, and in the presence of 2 mM Ca^{2+}, no cleavage of the second site could be detected (data not shown). The identity of these cleavage sites to those reported by Takahashi et al. (1986) was confirmed by N-terminal microsequencing of the 25- and 54-kDa fragments. It has been suggested that the second thrombin cleavage is responsible for the inactivation of FXIIIa (Takahaski et al., 1986). When rFXIII was incubated with bovine thrombin under conditions similar to those described by these authors (i.e., Tris–saline, RT), there was a loss of rFXIII activity following the peak activation. This loss of activity did not correlate well with the appearance of 25- and 54-kDa fragments but was accompanied by a visible precipitate (data not shown). No explanation for this phenomenon can be offered except that in our laboratory stability of rFXIIIa has been found to be highly dependent on rFXIIIa concentration and buffer composition with TANEP buffer being especially favorable for maintenance of rFXIIIa activity (see below).

A time course for rFXIII activation by human thrombin (10 units/mg rFXIII) performed in TANEP buffer is shown in Figure 7. Full activation was achieved within 3 min, and no inactivation was detected during the time course. When a similar time course was performed at a much higher thrombin to rFXIII ratio (180 units of thrombin/mg of rFXIII), no inactivation was detected even after a 3-h incubation time (data not shown).

Hornyak et al. (1989) have recently observed that acquisition of FXIII activity proceeded faster than the rate of thrombin activation cleavage. Their results indicated that a fully active dimer can consist of one proteolytically cleaved subunit and one zymogen subunit (aa′) and need not be composed of two thrombin-cleaved subunits (a'_2); i.e., FXIII appears to exhibit half of the sites reactivity as proposed by Chung et al. (1974). Interestingly, when a time course of rFXIII activation by human thrombin was performed, a 1:1 distribution of the a to a′ subunit was found to coincide with approximately 75% of the peak rFXIII activity (Figure 7). If it is assumed that the activation cleavage is random (i.e., that the rate of the a subunit activation cleavage is equal for both the a_2 and aa′ dimers), it follows that, when the concentrations of the a and a′ subunits are equal, a simple binomial distribution of the a and a′ subunits [i.e., $(a + a')^2$] will yield a ratio a_2:aa′:a'_2 of 1:2:1, and thus, 75% of the dimers will have been activated. This result is therefore consistent with the observations of Hornyak et al. (1989) and Chung et al. (1974).

Cross-Linking Activity in Plasma Clots. In order to confirm that rFXIII can function as a fibrin stabilizing factor, the cross-linking patterns of clots derived from human FXIII

deficient plasma supplemented with rFXIII were compared with the cross-linking pattern of normal human plasma clots. PAGE analysis of FXIII-deficient plasma clots (Figure 8, lanes b and c) indicated that there was no significant fibrin α-chain cross-linking and that the major proportion of fibrin γ-chains were not cross-linked (note the small amount of fibrin γ-chain dimers present indicates that this plasma was deficient but not devoid of FXIII activity). Supplementation of as little as 2 μg of rFXIII restored the normal fibrin cross-linking pattern of FXIII-deficient plasma (compare lanes d and i). This concentration of rFXIII is functionally equivalent to 10 μg of FXIII (a_2) per milliliter of whole plasma—the mean value for normal plasma being 15 μg/mL FXIII (as a_2 equivalent; McDonagh, 1987). Supplementation of rFXIII in concentrations in excess of that found in normal plasma did not appear to affect the fibrin cross-linking pattern observed by SDS-PAGE. The effect of rFXIII on the extent of fibrin α-chain cross-linking could not be quantitated, because the high molecular weights of the resulting aggregates effectively excluded them from entering the gel.

Acknowledgments

We thank the following co-workers for their expert technical assistance: Jay Gambee for the amino acid analysis; Sherri Osborn for the gas-phase microsequencing; Lin Phan, Bob Mills, John Fry, and Bob Dedinsky for their efforts during the fermentations and purifications; Dee Ann Curtis and Mason Bailey for developing the rFXIII and yeast antibodies. Special thanks to Akitada Ichinose for providing ZymoGenetics with the clone for the human FXIII a subunit and to Earl Davie for helpful discussions and encouragement in this project.

Registry No. FXIII, 9013-56-3.

References

Alber, T., & Kawasaki, G. (1982) *J. Mol. Appl. Genet. 1*, 419–434.

Bale, M. D., & Mosher, D. F. (1986) *Biochemistry 25*, 5667–5673.

Beggs, J. D. (1978) *Nature (London) 275*, 104–107.

Bohn, H. (1978) *Mol. Cell. Biochem. 20*, 67–75.

Carrell, N. A., Erickson, H. P., & McDonagh, J. (1989) *J. Biol. Chem. 264*, 551–556.

Chung, S. I., Lewis, M. S., & Folk, J. E. (1974) *J. Biol. Chem. 249*, 940–950.

Creeth, J. M., & Knight, C. G. (1965) *Biochim. Biophys. Acta 102*, 549–558.

Curtis, C. G., & Lorand, L. (1976) *Methods Enzymol. 45*, 177–191.

Curtis, C. G., Stenberg, P., Chou, C.-H. J., Gray, A., Brown, K. L., & Lorand, L. (1973) *Biochem. Biophys. Res. Commun. 52*, 51–58.

Curtis, C. G., Brown, K. L., Credo, R. B., Domanik, R. A., Gray, A., Stenberg, P., & Lorand, L. (1974a) *Biochemistry 13*, 3774–3780.

Curtis, C. G., Stenberg, P., Brown, K. L., Baron, A., Gray, A., Simpson, I., & Lorand, L. (1974b) *Biochemistry 13*, 3257–3263.

de Haen, C., Easterly, R. A., & Teller, D. C. (1983) *Biopolymers 22*, 1133–1143.

Duckert, F. (1972) *Ann. N.Y. Acad. Sci. 202*, 190–198.

Eghtedarzadeh, M. K., & Henikoff, S. (1986) *Nucleic Acids Res. 14*, 5115.

Folk, J. E. (1980) *Annu. Rev. Biochem. 49*, 517–531.

Folk, J. E., & Finlayson, J. S. (1977) *Adv. Protein Chem. 31*, 1–33.

Francis, R. R., McDonagh, J., & Mann, K. G. (1986) *J. Biol. Chem. 261*, 9787–9792.

Greenberg, C. S., Achyuthan, K. E., & Fenton, J. W., II (1987) *Blood 69*, 867–871.

Greenberg, C. S., Achyuthan, K. E., Rajagopalan, S., & Pizzo, S. (1988) *Arch. Biochem. Biophys. 262*, 142–148.

Grundman, U., Amana, E., Zettlmeissl, G., & Kupper, H. A. (1986) *Proc. Natl. Acad. Sci. U.S.A. 83*, 8024–8028.

Hornyak, T. J., Bishop, P. D., & Shafer, J. A. (1989) *Biochemistry 28*, 7326–7332.

Ichinose, A., & Aoki, N. (1982) *Biochim. Biophys. Acta 706*, 158–164.

Ichinose, A., McMullen, B. A., Fujikawa, K., & Davie, E. W. (1986a) *Biochemistry 25*, 4633–4638.

Ichinose, A., Hendrickson, L. E., Fujikawa, K., & Davie, E. W. (1986b) *Biochemistry 25*, 6900–6906.

Kitchens, C. S., & Newcomb, T. F. (1979) *Medicine 58*, 413–429.

Kozak, M. (1981) *Nucleic Acids Res. 9*, 5233–5252.

Kurjan, J., & Herskowitz, I. (1982) *Cell 30*, 933–943.

Lewis, S. D., Janus, T. J., Lorand, L., & Shafer, J. A. (1985) *Biochemistry 24*, 6772–6777.

Lorand, L., & Konishi, K. (1964) *Arch. Biochem. Biophys. 105*, 58–67.

Lorand, L., Lockridge, O. M., Campbell, L. K., Myhrman, R., & Bruner-Lorand, J. (1971) *Anal. Biochem. 44*, 221–231.

Lorand, L., Gray, A. J., Brown, K., Credo, R. B., Curtis, C. G., Domanik, R. A., & Stenberg, P. (1974) *Biochem. Biophys. Res. Commun. 56*, 914–922.

Lorand, L., Losowsky, M. S., & Miloszewski, K. J. M. (1980) *Prog. Hemostasis Thromb. 5*, 245–290.

Matsudaira, P. (1987) *J. Biol. Chem. 262*, 10035–10038.

McDonagh, J. A. (1987) in *Hemostasis and Thrombosis* (Colman, R. W., Hirsh, J., Marder, V. J., & Salzman, E. W., Eds.) pp 289–300, J. B. Lippinscott, Philadelphia.

Mimura, J., Kimura, S., & Aoki, N. (1986) *J. Clin. Invest. 77*, 1006–1013.

Mosher, D. F. (1975) *J. Biol. Chem. 250*, 6614–6621.

Mosher, D. F., & Schad, P. E. (1979) *J. Clin. Invest. 64*, 781–787.

Perkins, S. J. (1986) *Eur. J. Biochem. 157*, 169–180.

Perrin, F. (1936) *J. Phys. Radium 7*, 1–11.

Pilz, I., & Czerwenka, G. (1973) *Makromol. Chem. 170*, 185–190.

Russell, D. W., Smith, M., Cox, D., Williamson, V. M., & Young, E. T. (1983) *Nature (London) 304*, 652–564.

Sakata, Y., & Aoki, N. (1980) *J. Clin. Invest. 65*, 290–297.

Sakata, Y., & Aoki, N. (1981) *J. Clin. Invest. 69*, 536–542.

Schwartz, M. L., Pizzo, S. V., Hill, R. L., & McKee, P. A. (1971) *J. Biol. Chem. 246*, 5851–5854.

Schwartz, M. L., Pizzo, S. V., Hill, R. L., & McKee, P. A. (1973) *J. Biol. Chem. 248*, 1395–1407.

Senear, D. F., & Teller, D. C. (1981) *Biochemistry 20*, 3076–3083.

Skrzynia, C., Reisner, H. M., & McDonagh, J. (1982) *Blood 60*, 1089.

Swanson, E., Teller, D. C., & de Haen, C. (1980) *J. Chem. Phys. 72*, 1623–1628.

Tagaki, T., & Doolittle, R. F. (1974) *Biochemistry 13*, 750–756.

Takahashi, N., Takahashi, Y., & Putnam, F. W. (1986) *Proc. Natl. Acad. Sci. U.S.A. 83*, 8019–8023.

Tamaki, T., & Aoki, N. (1981) *Biochim. Biophys. Acta 661*, 280–286.

Tamaki, T., & Aoki, N. (1982) *J. Biol. Chem. 257*, 14767–14772.
Teller, D. C. (1973) *Methods Enzymol. 27D*, 346–441.
Teller, D. C., Swanson, E., & de Haen, C. (1979) *Methods Enzymol. 61H*, 103–124.
Thim, L., Hansen, M. T., Norris, K., Hoegh, I., Boel, E., Forstrom, J., Ammerer, G., & Fiil, N. (1986) *Proc. Natl. Acad. Sci. U.S.A. 83*, 6766–6770.
Towbin, H., Staehelin, T., & Gordon, J. (1979) *Proc. Natl. Acad. Sci. U.S.A. 76*, 4350–4356.
von Heijne, G. (1985) *J. Mol. Biol. 184*, 99–105.
von Heijne, G. (1986) *Nucleic Acids Res. 148*, 4683–4690.
Yphantis, D. A. (1964) *Biochemistry 3*, 297–317.
Zoller, M. J., & Smith, M. (1984) *DNA 3*, 479–488.

Effect of Tubulin Binding and Self-Association on the Near-Ultraviolet Circular Dichroic Spectra of Colchicine and Analogues†

Renee M. Chabin, Francisco Feliciano, and Susan Bane Hastie*
Department of Chemistry, State University of New York, Binghamton, New York 13901
Received August 15, 1989; Revised Manuscript Received October 19, 1989

ABSTRACT: Near-UV circular dichroic (CD) spectra of three colchicine analogues that differ at the C-10 position have been obtained in the presence and absence of tubulin. All three colchicine analogues show dramatic alterations in the low-energy near-UV CD band upon tubulin binding that cannot be mimicked by solvent, but in no event does the rotational strength of the CD band decrease to nearly zero as in the case of colchicine [Detrich, H. W., III, Williams, R. C., Jr., Macdonald, T. L., & Puett, D. (1981) *Biochemistry 20*, 5999–6005]. The effect of self-association of colchicine and one of the C-10 analogues, thiocolchicine, on the near-UV CD band was also investigated. A qualitative similarity was seen between the near-UV CD spectra of colchicine and thiocolchicine dimers and the spectra of these molecules bound to tubulin. These observations support the previous suggestion that ligands bound to the colchicine site on tubulin may be interacting with an aromatic amino acid in the colchicine binding site [Hastie, S. B., & Rava, R. P. (1989) *J. Am. Chem. Soc. 110*, 6993–7001].

Colchicine binding to tubulin, a 100 000-dalton protein which is the major protein component of the microtubule, is accompanied by ligand spectral alterations that are unique to tubulin binding and have resisted conventional explanation. [For reviews of the colchicine–tubulin association, see Brossi et al. (1988) and Luduena (1979).] The near-UV absorption spectrum of colchicine is a broad band that occurs at lower energy than tubulin absorption (λ_{max} = 353 nm in aqueous solution); the differences in energies of the tubulin and colchicine absorption spectra allow for examination of low-energy colchicine electronic spectra without interference by tubulin. Furthermore, the colchicine–tubulin complex, although noncovalent, dissociates so slowly that it is considered to be essentially irreversible, and thus spectra of the complex can be examined in the absence of unbound species.

The near-UV absorption band of colchicine is composed of two π–π^* transitions that are primarily located on the tropone C ring, and tubulin binding alters at least one of these transitions in a manner that has not yet been precisely duplicated in the absence of the protein (Hastie & Rava, 1989). The spectral changes in colchicine bound to tubulin are manifested in the absorption, fluorescence, and circular dichroic spectra of this low-energy absorption band. The overall absorption band of colchicine shifts to higher energy when the solvent dielectric constant is decreased; tubulin binding results in a small red shift in the absorption band (Bhattacharyya & Wolff, 1974). Tubulin binding also induces a dramatic enhancement of colchicine fluorescence (λ_{ex} = 350 nm, λ_{em} = 440 nm, ϕ = 0.03; Bhattacharyya & Wolff, 1974) that is not the result of simple hydrophobic effects, as the quantum yield of colchicine in aqueous solution and in low dielectric constant solvents is so low that the luminescence is difficult to detect. The sole condition that has been found so far to partially mimic tubulin-bound colchicine fluorescence is increased viscosity (Bhattacharyya & Wolff, 1984), leading to the hypothesis that tubulin binding serves to "immobilize" colchicine.

Perhaps the most dramatic change in colchicine's electronic spectra upon tubulin binding is observed by circular dichroism (CD).[1] The CD spectrum of colchicine in aqueous solution displays two negative bands in the 250–400-nm region of the spectrum (Hrbek et al., 1982). The band at 340 nm ($[\theta] \sim -34\,000$ deg·cm^2/dmol; Detrich et al., 1981) has been shown to arise primarily from the interaction of the tropone C ring with the trimethoxyphenyl A ring (Yeh et al., 1988), which are oriented in an "S" biaryl configuration with a dihedral angle of about 53° (Lessinger & Margulis, 1978). When colchicine is bound to tubulin and free ligand removed, the rotational strength of the 340-nm band is reduced to nearly zero (Detrich et al., 1981).

At least two suggestions have been put forth to explain the loss of the 340-nm CD band in the colchicine–tubulin complex. One suggestion is that the colchicine binding site on tubulin

† This work was supported in part by the National Science Foundation (ROW DMB 87 07360) and by a BRSG Grant (SO7RR07149-15) awarded by the Biomedical Research Support Grant Program Division of Research Resources, National Institutes of Health.

[1] Abbreviations: CD, circular dichroism; Pipes, piperazine-*N*,*N*′-bis(2-ethanesulfonic acid); EGTA, ethylene glycol bis(β-aminoethyl ether)-*N*,*N*,*N*′,*N*′-tetraacetic acid; PMEG buffer, 0.1 M Pipes, 1 mM $MgSO_4$, 2 mM EGTA, and 0.1 mM GTP, pH 6.90 at 23 °C.

0006-2960/90/0429-1869$02.50/0